PHYSICAL REVIEW C **84**, 061304(R) (2011)

Exploring the anomaly in the interaction cross section and matter radius of ^{23}O

R. Kanungo,[1,*] A. Prochazka,[2,3] M. Uchida,[1] W. Horiuchi,[4] G. Hagen,[5,6] T. Papenbrock,[5,6] C. Nociforo,[2] T. Aumann,[7,2] D. Boutin,[3] D. Cortina-Gil,[8] B. Davids,[9] M. Diakaki,[10] F. Farinon,[2,3] H. Geissel,[2] R. Gernhäuser,[11] J. Gerl,[2] R. Janik,[12] Ø. Jensen,[13] B. Jonson,[14] B. Kindler,[2] R. Knöbel,[2,3] R. Krücken,[11] M. Lantz,[14] H. Lenske,[3] Y. Litvinov,[2,15] B. Lommel,[2] K. Mahata,[2] P. Maierbeck,[11] A. Musumarra,[16] T. Nilsson,[14] C. Perro,[1] C. Scheidenberger,[2] B. Sitar,[12] P. Strmen,[12] B. Sun,[2,17] Y. Suzuki,[4,18] I. Szarka,[12] I. Tanihata,[19] H. Weick,[2] and M. Winkler[2]

[1]*Astronomy and Physics Department, Saint Mary's University, Halifax, Nova Scotia B3H 3C3, Canada*
[2]*GSI Helmholtzzentrum für Schwerionenforschung, D-64291 Darmstadt, Germany*
[3]*Justus-Liebig University, D-35392 Giessen, Germany*
[4]*RIKEN Nishina Center, Wako, Saitama 351-0918, Japan*
[5]*Physics Division, Oak Ridge National Laboratory, Oak Ridge, Tennessee 37831, USA*
[6]*Department of Physics and Astronomy, University of Tennessee, Knoxville, Tennessee 37996, USA*
[7]*Institut für Kernphysik, Technische Universität Darmstadt, D-6489 Darmstadt, Germany*
[8]*Universidad de Santiago de Compostela, E-15706 Santiago de Compostella, Spain*
[9]*TRIUMF, Vancouver, British Columbia V6T 2A3, Canada*
[10]*National Technical University, Athens, Greece*
[11]*Physik Department E12, Technische Universität München, D-85748 Garching, Germany*
[12]*Faculty of Mathematics and Physics, Comenius University, SK-84215 Bratislava, Slovakia*
[13]*Department of Physics and Center of Mathematics for Applications, University of Oslo, N-0316 Oslo, Norway*
[14]*Chalmers University of Technology, Göteborg, SE 412-916, Sweden*
[15]*Max-Planck-Institut für Kernphysik, Saupfercheckweg 1, D-69117 Heidelberg, Germany*
[16]*Universita' di Catania, I-95153 Catania, Italy*
[17]*School of Physics and Nuclear Energy Engineering, Beihang University, 100191 Beijing, People's Republic of China*
[18]*Department of Physics, Niigata University, Niigata 950-2181, Japan*
[19]*Research Center for Nuclear Physics (RCNP), Osaka University, Mihogaoka, Ibaraki, Osaka 567 0047, Japan*

(Received 17 September 2011; published 21 December 2011)

New measurements of the interaction cross sections of ^{22,23}O at 900A MeV performed at the GSI, Darmstadt are reported that address the unsolved puzzle of the large cross section previously observed for ^{23}O. The matter radii for these oxygen isotopes extracted through a Glauber model analysis are in good agreement with the new predictions of the *ab initio* coupled-cluster theory reported here. They are consistent with a ^{22}O + neutron description of ^{23}O as well.

DOI: 10.1103/PhysRevC.84.061304 PACS number(s): 25.60.Dz, 21.10.Gv, 21.60.De, 27.30.+t

The nucleon magic numbers are the fundamental basis for the concept of nucleons being arranged in a shell structure. While the distributions of nucleons in stable nuclei are fairly well understood, the neutron-rich nuclei show signatures of unconventional behavior. Of particular interest is the region around the new magic number $N = 16$ [1–3], at the neutron drip line that is a new benchmark point. Here, the nucleus ^{23}O plays a special role as a large enhancement in the interaction cross section was observed for ^{22}N, ^{23}O, and ^{24}F [1]. This leads to a large matter radius which was thought to reflect the formation of a neutron halo. However, the prediction by a core $(^{22}\mathrm{O}) + (2s_{1/2})$ neutron halo model was much lower than the data, and the matter distribution of ^{23}O remained an unsolved puzzle, a challenge for all models of nuclear structure.

The purpose of this Rapid Communication is to address this crucial issue by measuring the interaction cross section and reliably extracting the root-mean-square radii in order to reach a conclusive understanding of ^{23}O. The new observations resolve the existing anomaly, showing a smaller cross section consistent with both new *ab initio* model predictions presented here, and a ^{22}O core + neutron description.

There are several indications of a subshell gap at $N = 14$ in the oxygen isotopes. First, the 2^+ excitation energy of 3.199(8) MeV in ^{22}O [4,5] is large. Second, proton inelastic scattering of ^{22}O [6] revealed a small deformation parameter $\beta = 0.26 \pm 0.04$. This subshell gap suggests that the ^{23}O ground state could have a large component of a single-particle configuration with a $2s_{1/2}$ valence neutron. The nuclear and Coulomb breakup measurements of one-neutron removal from ^{23}O reported the $2s_{1/2}$ spectroscopic factors of 0.97 ± 0.19 [7,8] and 0.78 ± 0.13 [9], respectively. A significant yield of the ^{22}O excited state (3.2, 5.8 MeV) components was observed in the nuclear breakup. However, the $^{22}\mathrm{O} + n(2s_{1/2})$ description in which the ^{22}O core is considered to be identical to the bare ^{22}O nucleus severely underpredicted the measured interaction cross section [1]. It was therefore proposed [10] that the ^{22}O core within ^{23}O is possibly modified and enlarged compared to the bare ^{22}O nucleus, giving rise to a larger interaction cross section. The relatively narrow momentum distribution of the two-neutron removal fragment ^{21}O from ^{23}O [11] suggested that ^{23}O might have some probability of two neutrons occupying the $2s_{1/2}$ orbital. However, this is not consistent with the reported $2s_{1/2}$ spectroscopic factors.

*ritu@triumf.ca

The energy gap at $N = 14$ in ^{23}O was found to be 2.79(13) MeV from fragmentation of ^{26}Ne, populating the resonance in ^{23}O at 45(2) keV above the $^{22}\mathrm{O} + n$ threshold [12]. This was considered to be the $5/2^+$ excited state in ^{23}O. The higher-lying resonance at 1.3 MeV above the neutron threshold observed in the $^{22}\mathrm{O}(d, p)$ reaction [13] was understood to be the $3/2^+$ excited state that shows a 4.00(2) MeV gap between the $2s_{1/2}$ and $1d_{3/2}$ orbitals.

Recently, the neutron knockout of $^{24}\mathrm{O} \rightarrow ^{23}$ O revealed a large two-neutron spectroscopic factor of 1.74 ± 0.19, exhausting the s-orbital occupancy with no significant observable d component establishing a spherical shell closure at $N = 16$ [2,14]. The neutron-unbound excited state of ^{24}O at 4.72(11) MeV [3], considered to be the first 2^+ state, is also supportive of ^{24}O being a doubly-magic nucleus. These findings are difficult to reconcile with the unusually large interaction cross section of ^{23}O reported in Ref. [1]. Such an anomaly may point to unknown structure effects to which the breakup reactions may not be sensitive. It is of utmost importance to address the issue since the neutron-rich oxygen isotopes form crucial benchmark points for understanding the evolution of the shell structure in neutron-rich regions. It has been shown that three-body forces play an important role to define the drip line of the oxygen isotopes [15].

We performed an experiment to measure the interaction cross sections of ^{22,23}O at the fragment separator FRS at GSI [16]. The experiment layout is shown in Fig. 1 of Ref. [17]. The measurement is done by the method of transmission where the total interaction cross section for reactions in the target is given by $\sigma_I = (-1/t)\ln(R_{\mathrm{in}}/R_{\mathrm{out}})$. The transmission ratio is $R_{\mathrm{in}} = N_{\mathrm{in}}^f/N_{\mathrm{in}}^i$, where N_{in}^i and N_{in}^f are the number of ^{A}O before and after the target, respectively. R_{out} is the same but for an empty target and t is the number of target nuclei per unit area.

The ^{A}O nuclei were produced from the fragmentation of a $1A$ GeV ^{48}Ca beam interacting with a 6.3 g/cm^2 thick Be target. The fragmentation products were separated and identified using the first half of the FRS, where plastic scintillator detectors placed at the two dispersive foci, F1 and F2, measured the time of flight (TOF). The precise beam position measured using time projection chamber (TPC) detectors placed at F2 and the magnetic rigidity of the FRS provide information on the mass-to-charge ratio (A/Q) of the fragments. A multisampling ionization chamber (MUSIC) placed at F2 measured the energy loss (with a 1σ resolution of $\sim$3%), providing the Z identification of the ^{A}O beam.

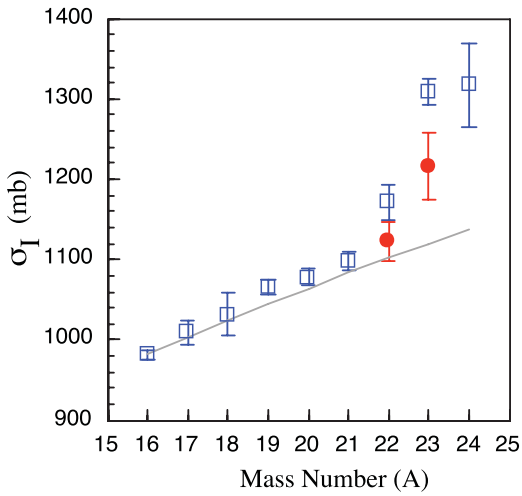

FIG. 1. (Color online) The interaction cross section of $^A\mathrm{O} + \mathrm{C}$ as a function of the mass number. The circles represent the present data, and the squares are from Ref. [1]. The line shows the $A^{1/3}$ dependence normalized to ^{16}O.

A 4.046 g/cm^2 thick carbon reaction target was placed at F2. The second half of the fragment separator consists of a dispersive focus at F3 and an achromatic focus at F4. The ion optics mode was selected to match the dispersion of the first half with the second half. The magnetic rigidity of the second half was set to transport the unreacted ^{A}O to the final focus (F4). Here products were identified in A/Q using magnetic rigidity, TOF between plastic scintillators at F2 and F4, and position measurement using TPC detectors placed at F4. Two MUSIC detectors were placed at F4 to measure the energy loss of the products after the reaction target. Events that were observed to be consistent with $Z = 8$ in either MUSIC were counted as unreacted events. To account for losses occurring due to reactions in other materials in the setup, data were also collected with an empty target frame. The position and angle of the incident beam before the target at F2 were restricted from beam tracking measurements such that transmission from F2 to F4 was a constant within the selected phase space.

The measured interaction cross section at $\sim 900A$ MeV is shown in Fig. 1 as a function of the mass number of the oxygen isotopes, with the filled circles showing the present data from Table I. The open squares are the data of Ref. [1]. It is seen that the present data of ^{23}O are smaller than that reported earlier. The total uncertainties shown are dominated by statistics. The uncertainty from contamination of the incoming beam (for Z and A) was at most $\sim$0.9%, and that from the target thickness was 1.2%. The transmission uncertainty was $\sim$1.5%. The cross section for ^{22}O is also slightly smaller than previously reported. The cross section for the isotope ^{28}Ne extracted from the same data results in 1271 ± 35 mb, which agrees within uncertainty with the value of 1244 ± 44 mb reported in Ref. [18]. The interaction cross section of ^{23}O reported here is $\sim$8%–9% larger than ^{22}O, which may not be sufficient to be classified as a one-neutron halo (^{11}Be, a halo, has an $\sim$16% larger cross section than ^{10}Be). This is consistent with the fact that the one-neutron separation energy of ^{23}O, $S_n = 2.7$ MeV, is quite large, which inhibits the tunneling of the wave function into the classically forbidden region to form a halo.

The root-mean-square (rms) matter radius is extracted by interpreting the data in the framework of the Glauber model, including the higher-order terms that are missing in

TABLE I. Measured interaction cross sections and the root-mean-square point matter radii (R_{rms}^m) for $^{22-23}$O using Fermi (Fermi) and harmonic oscillator (HO) densities.

Isotope	$\sigma_I(\Delta\sigma)$ (mb)	$\Delta\sigma$(Stat.) (mb)	$\Delta\sigma$(Syst.) (mb)	$R_{\mathrm{rms}}^{m(\mathrm{Fermi})}$ (fm)	$R_{\mathrm{rms}}^{m(\mathrm{HO})}$ (fm)
^{22}O	1123(24)	18.5	15.3	2.75(0.15)	2.75(0.07)
^{23}O	1216(41)	33.1	24.7	2.95(0.23)	2.97(0.11)

the usual optical approximation [19,20]. The matter density was considered to be a Fermi density of the form $\rho(r) = \rho_0/\{1 + \exp[(r - R)/a]\}$, where $R = r_0 A^{1/3}$. The calculated cross sections for different values of radius ($r_0 \sim 0.8-1.4$ fm) and diffuseness ($a \sim 0.3-0.7$ fm) parameters are shown by the different solid points in Figs. 2(a) and 2(b). Calculations using separate neutron and proton Fermi functions were found to yield similar rms radii. The rms matter radius that can reproduce the experimental cross section is found to be 2.75 ± 0.15 fm for ^{22}O while for ^{23}O a radius of 2.95 ± 0.23 fm is extracted [Table I, shown by the horizontal arrows in Figs. 2(a) and 2(b)]. To investigate any model dependence we also extract the rms radii with a harmonic oscillator form of density [18]. The radii extracted shown by the solid line (open points) in Figs. 2(a) and 2(b) are consistent with those using Fermi density (Table I). Since the oscillator width is the only parameter here, the uncertainty of the radius is found to be slightly smaller.

A subshell closure at $N = 14$ has been discussed for ^{22}O which, in a simplistic model, allows us to describe ^{23}O being composed of a ^{22}O core + neutron, and we interpret next the interaction cross section in a few-body Glauber model framework [21]. The core ^{22}O is considered to have the same Fermi density profile as the bare ^{22}O nucleus mentioned above. The wave functions of the valence neutron are calculated with a Woods-Saxon bound state potential ($r_0 = 1.27$ fm and $a = 0.67$ fm), where the depth is varied to reproduce the effective neutron separation energy. The dashed line in Fig. 2(c) shows the calculated cross sections with the valence neutron in the $2s_{1/2}$ orbital. The cross section shown is calculated as a function of the rms matter radius of ^{22}O (from Table I). The horizontal shaded area is the measured interaction cross section of ^{23}O. The overlap of the calculated values with this shaded region shows consistency with data. It is seen therefore that ^{23}O can be described by a ^{22}O core + $2s_{1/2}$ neutron. The dotted line shows a similar calculation but for the neutron in the $1d_{5/2}$ orbital and with the core ^{22}O in its 2^+ excited state. The density of ^{22}O in its 2^+ state was assumed to be the same as the ground state.

To gain a better understanding, we perform *ab initio* coupled-cluster (CC) [22] computations. This method is uniquely suited for describing nuclei with closed neutron and proton subshells and their neighbors. Within particle-removed CC theory, the ground state of ^{23}O is described as a superposition of $1h$ and $1p2h$ excitations on top of the correlated ground state of ^{24}O [23]. We employ a low-momentum version of the nucleon-nucleon interaction from chiral effective field theory [24] that results from a similarity renormalization group transformation [25] and is characterized by a momentum cutoff λ. We work with the intrinsic Hamiltonian, i.e., the kinetic energy of the center of mass is subtracted from the total kinetic energy. As a result, the coupled-cluster wave function factorizes with a high degree of accuracy into a product of an intrinsic wave function and a Gaussian for the center of mass [26]. In this framework we compute the density of the ^{23}O ground state. The intrinsic density, i.e., the density with respect to the center of mass, results from a deconvolution with respect to the Gaussian center-of-mass wave function. It enters the computation of the interaction cross section and the matter

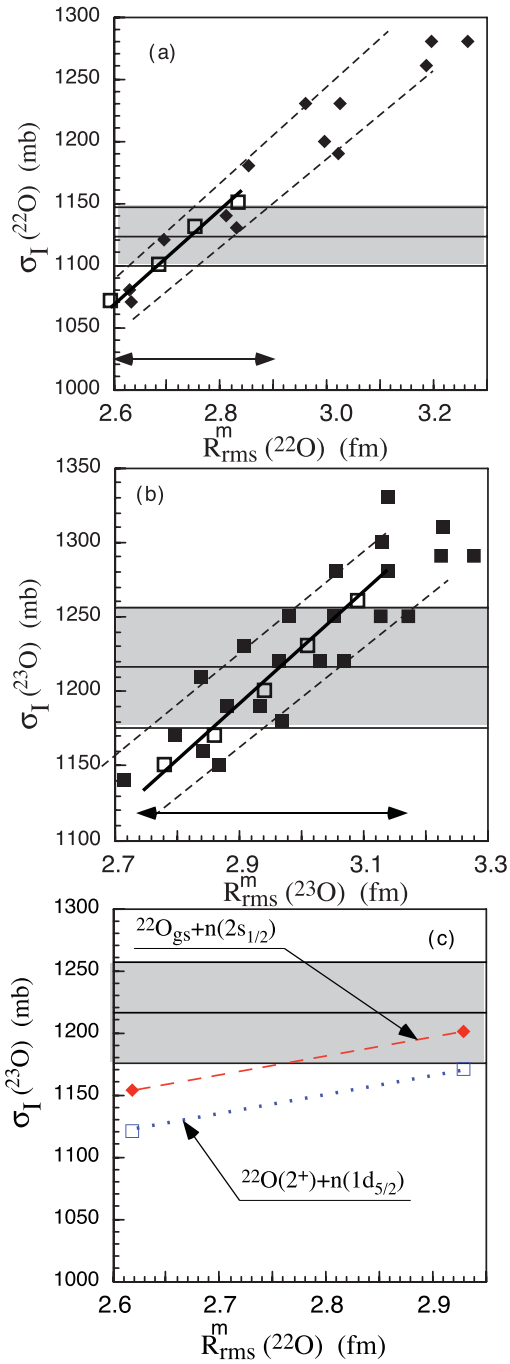

FIG. 2. (Color online) The interaction cross-section data for (a) ^{22}O + C and (b) ^{23}O + C (shaded regions). The filled squares are Glauber model calculations with Fermi density parameters r_0 and a shown as a function of $R^m_{\rm rms}(^A{\rm O})$. The dotted lines show a guide to the eye for determining the limits of $R^m_{\rm rms}$ consistent with the data. The solid lines guiding the open squares, are calculations with harmonic oscillator density. (c) The interaction cross-section data for ^{23}O + C (shaded region). The dashed (dotted) line is a ^{22}O + n few-body Glauber model calculation for $2s_{1/2}$ ($1d_{5/2}$) orbitals as a function of different ^{22}O rms radii within uncertainty of the value quoted in Table I.

radii. Our model space consisted of 30 bound and continuum Woods-Saxon orbitals for the neutron, $l = 0$ and $l = 2$ partial

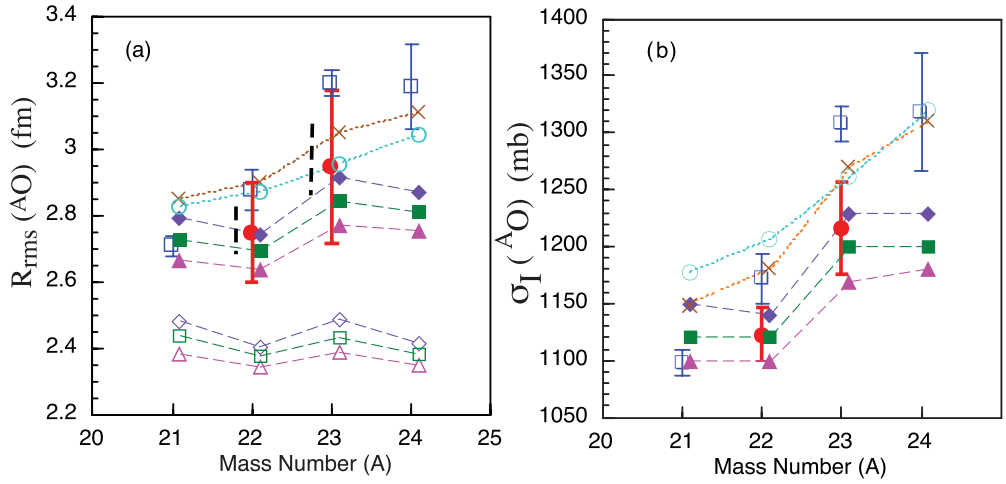

FIG. 3. (Color online) (a) The red filled circles show $R^{m(\mathrm{Fermi})}_{\mathrm{rms}}$, the dashed vertical line is $R^{m(\mathrm{HO})}_{\mathrm{rms}}$, and the blue open squares are R^{m}_{rms} from Ref. [1]. The diamonds/squares/triangles are coupled-cluster calculations with a cutoff parameter $= 4.0/3.8/3.6$ fm^{-1}, where the filled points are R^{m}_{rms} and the open points are proton rms radii, respectively. (b) The interaction cross section of ^{A}O + C as a function of the mass number. The red filled circles are present data, and the open squares are from Ref. [1]. The diamonds/squares/triangles are CC calculations with a cutoff parameter $= 4.0/3.8/3.6$ fm^{-1}. The cross marks (open circles) show results from Ref. [27] (Ref. [28]).

waves, and 17 major oscillator shells for the remaining neutron partial waves and the protons.

The computed point matter radii are in good agreement with our data [Fig. 3(a)]. Smaller values of the momentum cutoff lead to smaller radii. The relative uncertainties in the experimental radii are larger than those of the interaction cross sections due to the uncertainties in the Fermi density profiles. We also compare the cross sections calculated with density distributions from the coupled-cluster theory in Fig. 3(b). The cross sections with $\lambda = 4.0$ and 3.8 fm^{-1} are in good agreement with the data, while that with $\lambda = 3.6$ fm^{-1} is slightly below the 1σ error. The variation of the radii with the cutoff provides an estimate of the contributions of neglected short-ranged three-nucleon forces. The relative isotopic differences in radii from $^{21-24}$O depend only very weakly on the cutoff, suggesting it to probably have a weak dependence on three-nucleon forces. The results with densities from Ref. [27] which were generated by a Slater determinant in a mean-field potential are shown by the cross marks in (Fig. 3). The open circles (Fig. 3) show results with densities from a Skyrme-Hartree-Fock potential [28].

In conclusion, this work reports new measurements of the interaction cross sections of ^{22,23}O at 900A MeV. The new data for ^{23}O is consistent, within experimental errors, with a model of a ^{22}O core + valence neutron in the $2s_{1/2}$ orbital, thereby addressing the existing anomaly in its structure. Beyond this simplistic model, new coupled-cluster calculations reported here show excellent agreement with the present data. This shows the significant advancement made jointly by experiment and *ab initio* theories in reaching a conclusive understanding of the matter distribution in ^{23}O. The radii extracted are shown to be consistent for the different parametric density forms. The results show growth of neutron skin from ^{21}O to ^{23}O, but a large enhancement characteristic of a halo is not observed for ^{23}O.

The authors are thankful for the support of the GSI accelerator staff and the FRS technical staff for efficient running of the experiment. The support from NSERC for this work is gratefully acknowledged. This work was supported by the BMBF under Contract No. 06MT238, by the DFG cluster of excellence *Origin and Structure of the Universe*. This work was supported by the US Department of Energy, Grants No. DE-FG02-96ER40963 (University of Tennessee), and No. DE-FC02-07ER41457 (UNEDF SciDAC). This research used computational resources of the National Center for Computational Sciences. W.H. is supported by the Special Postdoctoral Researchers Program of RIKEN. We thank B. A. Brown for the providing us the values of Ref. [28].

[1] A. Ozawa, T. Kobayashi, T. Suzuki, K. Yoshida, and I. Tanihata, Phys. Rev. Lett. **84**, 5493 (2000); A. Ozawa *et al.*, Nucl. Phys. A **691**, 599 (2001).
[2] R. Kanungo *et al.*, Phys. Rev. Lett. **102**, 152501 (2009).
[3] C. R. Hoffman *et al.*, Phys. Lett. B **672**, 17 (2009).
[4] O. Sorlin, Nucl. Phys. A **685**, 186c (2001).
[5] M. Stanoiu *et al.*, Phys. Rev. C **69**, 034312 (2004).
[6] E. Becheva *et al.*, Phys. Rev. Lett. **96**, 012501 (2006).
[7] D. Cortina-Gil *et al.*, Phys. Rev. Lett. **93**, 062501 (2004).
[8] C. Rodriguez-Tajes *et al.*, Phys. Rev. C **82**, 024305 (2010).
[9] C. Nociforo *et al.*, Phys. Lett. B **605**, 79 (2005).
[10] R. Kanungo, I. Tanihata, and A. Ozawa, Phys. Lett. B **512**, 261 (2001).
[11] R. Kanungo *et al.*, Phys. Rev. Lett. **88**, 142502 (2002).

[12] A. Schiller *et al.*, Phys. Rev. Lett. **99**, 112501 (2007).
[13] Z. Elekes *et al.*, Phys. Rev. Lett. **98**, 102502 (2007).
[14] Ø. Jensen, G. Hagen, M. Hjorth-Jensen, and J. S. Vaagen, Phys. Rev. C **83**, 021305 (2011).
[15] T. Otsuka, T. Suzuki, J. D. Holt, A. Schwenk, and Y. Akaishi, Phys. Rev. Lett. **105**, 032501 (2010).
[16] H. Geissel *et al.*, Nucl. Instrum. Methods Phys. Res. B **70**, 286 (1992).
[17] R. Kanungo *et al.*, Phys. Rev. C **83**, 021302 (R) (2011).
[18] A. Ozawa, T. Suzuki, and I. Tanihata, Nucl. Phys. A **693**, 32 (2001).
[19] B. Abu-Ibrahim and Y. Suzuki, Phys. Rev. C **61**, 051601(R) (2000).
[20] W. Horiuchi, Y. Suzuki, B. Abu-Ibrahim, and A. Kohama, Phys. Rev. C **75**, 044607 (2007).
[21] B. Abu-Ibrahim, Y. Ogawa, Y. Suzuki, and I. Tanihata, Comput. Phys. Commun. **151**, 369 (2003).
[22] F. Coester, Nucl. Phys. **7**, 421 (1958); H. Kümmel, K. H. Lührmann, and J. G. Zabolitzky, Phys. Rep. **36**, 1 (1978).
[23] G. Hagen, T. Papenbrock, D. J. Dean, and M. Hjorth-Jensen, Phys. Rev. C **82**, 034330 (2010).
[24] D. R. Entem and R. Machleidt, Phys. Rev. C **68**, 041001 (2003).
[25] S. K. Bogner, R. J. Furnstahl, and R. J. Perry, Phys. Rev. C **75**, 061001 (2007).
[26] G. Hagen, T. Papenbrock, and D. J. Dean, Phys. Rev. Lett. **103**, 062503 (2009).
[27] B. Abu-Ibrahim, S. Iwasaki, W. Horiuchi, A. Kohama, and Y. Suzuki, J. Phys. Soc. Jpn. **78**, 044201 (2009).
[28] B. A. Brown, S. Typel, and W. A. Richter, Phys. Rev. C **65**, 014612 (2001).